Molecular g Values, Magnetic Susceptibility Anisotropies, Second Moment of the Charge Distribution, and Molecular Quadrupole Moments in Formic Acid[1]

S. G. Kukolich and W. H. Flygare

Contribution from the W. A. Noyes Chemical Laboratory, University of Illinois, Urbana, Illinois. *Received November 16, 1968*

Abstract: The high-field rotational Zeeman effect has been observed in formic acid. The molecular g values and anisotropies in the magnetic susceptibilities are $g_{aa} = -0.2797 \pm 0.006$, $g_{bb} = -0.0903 \pm 0.0006$, $g_{cc} = -0.0270 \pm 0.0006$, $2\chi_{aa} - \chi_{bb} - \chi_{cc} = (3.4 \pm 0.5) \times 10^{-6}$ erg/(G² mole), and $2\chi_{bb} - \chi_{aa} - \chi_{cc} = (9.4 \pm 0.3) \times 10^{-6}$ erg/(G² mole). Only the relative signs of the g values are determined experimentally. However, by comparing the calculated molecular quadrupole moments (for both all positive and all negative g values) with known values for other similar molecules, the above negative signs are conclusively assigned. The molecular quadrupole moments are $Q_{aa} = -(5.3 \pm 0.4) \times 10^{-26}$ esu cm², $Q_{bb} = +(5.2 \pm 0.4) \times 10^{-26}$ esu cm², and $Q_{cc} = +(0.1 \pm 0.4) \times 10^{-26}$ esu cm². The a axis is nearly along a line connecting the two oxygen atoms, and this axis makes an angle of 31.6° with the C=O bond direction. The b axis is also in the OCO plane. The diagonal elements in the total magnetic susceptibility tensor are $\chi_{aa} = -(18.8 \pm 0.8) \times 10^{-6}$ erg/(G² mole), $\chi_{bb} = -(16.8 \pm 0.8) \times 10^{-6}$ erg/(G² mole), and $\chi_{cc} = -(24.2 \pm 0.8) \times 10^{-6}$ erg/(G² mole). The diagonal elements in the paramagnetic susceptibility tensor are $\chi_{aa}^{p} = (28.8 \pm 0.1) \times 10^{-6}$, $\chi_{bb}^{p} = (106.5 \pm 0.1) \times 10^{-6}$, and $\chi_{cc}^{p} = (117.2 \pm 0.1) \times 10^{-6}$ all in units of erg/(G² mole). The diagonal elements in the second moment of the electronic charge distribution are $\langle a^2 \rangle = (26.6 \pm 0.3) \times 10^{-16}$ cm², $\langle b^2 \rangle = (7.7 \pm 0.3) \times 10^{-16}$ cm², and $\langle c^2 \rangle = (3.5 \pm 0.2) \times 10^{-16}$ cm².

The molecular Zeeman effect in diamagnetic molecules is proving to be a valuable tool in the study of the electronic charge distribution in molecules. The *first-order* molecular Zeeman effect leads to a measurement of the molecular g values in the principal inertial axis system. If the molecular structure is known, the molecular g values lead to a direct determination of the diagonal elements in the paramagnetic susceptibility tensor in the principal inertial axis system. The *second-order* molecular Zeeman effect leads to a direct measurement of the anisotropies in the total magnetic susceptibility tensor elements. The anisotropies in the total magnetic susceptibility can be combined with the first-order determined paramagnetic susceptibility elements to yield the anisotropies in the ground-state second moment of the electronic charge distribution. Furthermore, if the bulk or average magnetic susceptibility is known, each element in the total susceptibility and each diagonal element of the second moment of the electronic charge distribution can be obtained.

The *first-order* determined molecular g values can be combined with the *second-order* determined magnetic susceptibility anisotropies to obtain a direct measurement of the molecular quadrupole moments.

Previous studies of the rotational Zeeman effect has led to *first-order* measurement or the molecular g values[2] in several molecules. Hüttner and Flygare[3] have discussed the theory of molecular Zeeman effect, and they have pointed toward the use of microwave spectroscopy to obtain the *second-order* or magnetic susceptibility anisotropies in complex molecules. Hüttner, Lo, and Flygare[4] first demonstrated the observation of the *second-order* Zeeman effect in formaldehyde. Since then, the combination of high magnetic fields with high-resolution microwave spectroscopy has led to the measurement of the molecular g values, magnetic susceptibility anisotropies, and molecular quadrupole moments in several molecules. This paper contains the above results for formic acid. The formic acid results are then compared to similar molecules.

The Experiment and Data Analysis

The microwave spectrometer and high-field electromagnet have been described previously.[5] Briefly, the microwave spectrograph is a relatively standard high-resolution system with the high microwave frequencies phase stabilized to lower frequency oscillators. The magnet has either a 12 × 72 in. flat pole configuration or poles tapered to 2 in. over the full length of 72 in. $\Delta M_J = \pm 1$ transitions are observed when the magnetic field is perpendicular to the electric field of the microwaves. An X-band cell in a 1.1-in. gap allows a field of 27,000 G to be obtained. By rotating the X-band wave guide by 90°, the magnet gap can be reduced to 0.6 in. and fields up to 30,000 G are observed. The magnetic field is now parallel to the electric field of the microwaves leading to $\Delta M = 0$ transitions. The field is measured to an accuracy of better than 0.2% with a Rawson-Lush Type 920 rotating coil gaussmeter which is periodically calibrated with an nmr gaussmeter.

The zero-field microwave spectrum of formic acid has been studied in considerable detail.[6,7] The transitions studied in this experiment were the $0_{00} \rightarrow 1_{01}$ at 22,471.2 MHz, the $3_{12} \rightarrow 3_{13}$ at 9831.98 MHz, and the $5_{14} \rightarrow 5_{15}$ at 24,568.92 MHz. The spectra at high magnetic fields

(1) This work was partially supported by the Advanced Research Projects Agency Grant SD-131 to the Materials Research Laboratory at the University of Illinois.

(2) C. H. Townes and A. L. Schawlow, "Microwave Spectroscopy," McGraw-Hill Book Co., Inc., New York, N. Y., 1955.

(3) W. Hüttner and W. H. Flygare, *J. Chem. Phys.*, **47**, 4137 (1967).

(4) W. Hüttner, M. K. Lo, and W. H. Flygare, *ibid.*, **48**, 1206 (1968).

(5) W. H. Flygare, W. Huttner, R. L. Shoemaker, and P. D. Foster, *ibid.*, in press.

(6) R. Trambarulo, A. Clark, and C. Hearns, *ibid.*, **28**, 736 (1958).

(7) G. Erlandsson, *ibid.*, **28**, 71 (1958).

is expected to be dominated by the first-order Zeeman effect as in formaldehyde[4] and ketene.[8]

The theory of the rotational Zeeman effect in an asymmetric top has been given by Hüttner and Flygare.[3] The rotational energy levels of formic acid are expected to be governed by eq 28 in ref 3 which is

$$E(J, M_J) = -\frac{1}{2}\chi H^2 - \mu_0 \frac{M_J H}{J(J+1)} \sum_g g_{gg}\langle P_g^2\rangle - H^2\left[\frac{3M_J^2 - J(J+1)}{(2J-1)(2J+3)}\right]\left[\frac{1}{J(J+1)}\right] \times \sum_g (\chi_{gg} - \chi)\langle P_g^2\rangle \quad (1)$$

$\chi = {}^1/_3(\chi_{aa} + \chi_{bb} + \chi_{cc})$ is the average magnetic susceptibility with χ_{aa}, χ_{bb}, and χ_{cc} being the components along the principal inertial axes in the molecule. H is the external magnetic field, μ_0 is the nuclear magneton, J and M_J are the rotational quantum numbers, g_{gg} is the molecular g value along the gth principal inertial axis, and $\langle P_g^2\rangle$ is the average value of the squared rotational angular momentum along the gth principal inertial axis. The $-{}^1/_2\chi H^2$ term will cancel out in our observation of an energy difference. Thus, we can measure the absolute values of the three g values and two independent magnetic anisotropy parameters. The magnetic anisotropy components are

$$\chi_{aa} - \chi = \frac{1}{3}(2\chi_{aa} - \chi_{bb} - \chi_{cc})$$

$$\chi_{bb} - \chi = \frac{1}{3}(-\chi_{aa} + 2\chi_{bb} - \chi_{cc}) \quad (2)$$

$$\chi_{cc} - \chi = \frac{1}{3}(-\chi_{aa} - \chi_{bb} + 2\chi_{cc})$$

Only two of these equations are independent. We have written our least-squares program to give the values of $2\chi_{aa} - \chi_{bb} - \chi_{cc}$ and $2\chi_{bb} - \chi_{cc} - \chi_{aa}$. The third anisotropy component is the negative sum of the first two as the trace of the $\chi_{gg} - \chi$ is zero.

The high-field molecular Zeeman effect in the $5_{14} \rightarrow 5_{15}$ transition for both the $\Delta M = 0$ and $\Delta M = \pm 1$ transitions are shown in Figures 1 and 2. The $\Delta M = 0$ transition intensities are proportional to M^2. Thus, the intensities of the outer components are 25 ($M = \pm 5$) and progress from both sides with relative intensities 16 ($M = \pm 4$), 9 ($M = \pm 3$), 4 ($M = \pm 2$), and 1 ($M = \pm 1$) toward ν_0. The $M = \pm 5$, ± 4, ± 3, and ± 2 transitions are all evident in Figure 1. The pattern shown in Figure 1 is expected for a dominant first-order spectra. However, note that the spacings between the M components is compressed in the higher frequency $+|M| \rightarrow |M|$ components relative to the lower frequency $-|M| \rightarrow |M|$ components. This latter asymmetry is due to the anisotropies in the magnetic susceptibilities. These same effects are more evident in the $3_{13} \rightarrow 3_{12}$ transition shown in Figure 3. Accurate measurements of the transitions shown in Figure 1 are listed in Table I. The $5_{14} \rightarrow 5_{15}$ $\Delta M = \pm 1$ transitions are shown in Figure 2. The first-order spectra would lead to 20 lines; ten $\Delta M = +1$ and ten $\Delta M = -1$ transitions. The results in Figure 2 show only a partial resolution of the higher $\Delta M = +1$ series with respect to the lower frequency $\Delta M = -1$ series. Only the outer well-resolved components of each series are listed in Table I for the extraction of the data. Notice again that the higher frequency $\Delta M = +1$ components are compressed relative to the lower frequency $\Delta M = -1$ components.

We have used the data in Table I and eq 1 to extract the

(8) W. Huttner, W. H. Flygare, and P. D. Foster, *J. Chem. Phys.*, in press.

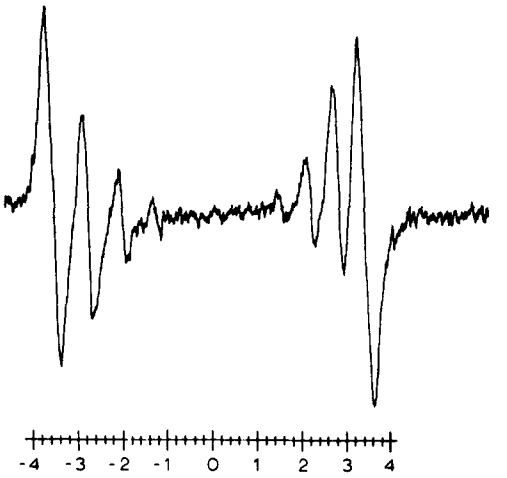

Figure 1. Recorder trace of the 5_{14}–5_{15}, $\Delta M = 0$ transitions in formic acid. The frequency scale is in MHz relative to the zero-field transition at 24,568.92 MHz. The frequencies are listed in Table I.

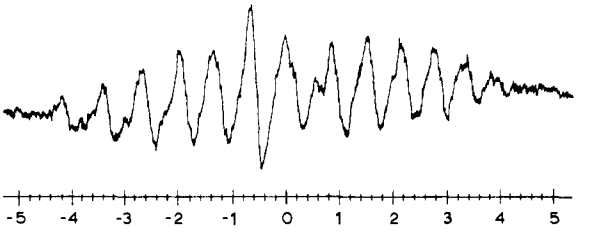

Figure 2. Recorder trace of the 5_{14}–5_{15}, $\Delta M = \pm 1$ transitions in formic acid (see Table I).

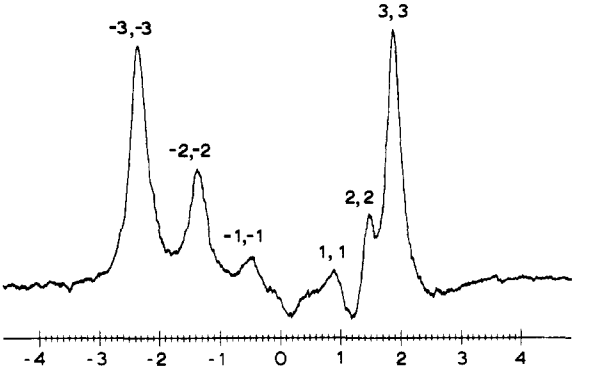

Figure 3. Recorder trace of the 3_{13}–3_{12}, $\Delta M = 0$ transitions in formic acid. The frequency scale is in MHz relative to the zero-field transition at 9831.98 MHz (see Table I).

Table I. Results of Measurements and Calculations for the Zeeman Effect in HCOOH[a]

ΔJ	$M \rightarrow M'$	Data	Calcd	Δ	H
0_{00}–1_{01}	$0 \rightarrow -1$	−1129	−1115	−14	25,350
	$0 \rightarrow 0$	−51	−48	−3	29,260
	$0 \rightarrow 1$	1149	1151	2	25,350
3_{13}–3_{12}	$-2 \rightarrow -3$	−3103	−3104	1	25,440
	$-1 \rightarrow -2$	−2334	−2339	5	25,440
	$0 \rightarrow -1$	−1655	−1654	−1	25,440
	$1 \rightarrow 0$	−1045	−1049	4	25,440
	$2 \rightarrow 1$	−515	−525	9	25,440
	$-3 \rightarrow -3$	−2371	−2385	14	29,270
	$-2 \rightarrow -2$	−1414	−1413	−1	29,270
	$-1 \rightarrow -1$	−554	−548	−6	29,270
	$1 \rightarrow 1$	866	866	0	29,270
	$2 \rightarrow 2$	1406	1413	−7	29,270
	$3 \rightarrow 3$	1857	1855	2	29,270
	$-2 \rightarrow -1$	612	617	−5	25,440
	$-1 \rightarrow 0$	1319	1320	−5	25,440
	$0 \rightarrow 1$	1952	1944	8	25,440
	$1 \rightarrow 2$	2497	2487	10	25,440
	$2 \rightarrow 3$	2969	2950	19	25,440
5_{15}–5_{14}	$-4 \rightarrow -5$	−4180	−4157	−23	25,360
	$-3 \rightarrow -4$	−3435	−3428	−7	25,360
	$-2 \rightarrow -3$	−2715	−2729	14	25,360
	$-1 \rightarrow 0$	−2040	−2061	21	25,360
	$0 \rightarrow 1$	−1400	−1424	24	25,360
	$-5 \rightarrow -5$	−3819	−3833	14	29,260
	$-4 \rightarrow -4$	−2931	−2944	13	29,260
	$-3 \rightarrow -3$	−2095	−2096	13	29,260
	$-2 \rightarrow -2$	−1296	−1289	−7	29,260
	$2 \rightarrow 2$	1522	1533	−11	29,260
	$3 \rightarrow 3$	2140	2137	3	29,260
	$4 \rightarrow 4$	2724	2700	24	29,260
	$5 \rightarrow 5$	3223	3223	0	29,260
	$-1 \rightarrow 0$	1115	1103	12	25,360
	$0 \rightarrow 1$	1720	1719	1	25,360
	$1 \rightarrow 2$	2305	2305	0	25,360
	$2 \rightarrow 3$	2865	2860	5	25,360
	$3 \rightarrow 4$	3395	3384	11	25,360
	$4 \rightarrow 5$	3855	3878	−23	25,360

[a] All frequencies are given in kHz as shifts from the zero-field frequencies. Δ is the difference between observed and calculated frequencies. H is the field in gauss.

Table II. The Molecular g Values and Magnetic Susceptibility Anisotropy Terms Obtained in Formic Acid[a]

$$g_{aa} = -0.2797 \pm 0.006$$
$$g_{bb} = -0.0903 \pm 0.0006$$
$$g_{cc} = -0.0270 \pm 0.0006$$
$$2\chi_{aa} - \chi_{bb} - \chi_{cc} = (3.4 \pm 0.5) \times 10^{-6} \text{ erg/(G}^2 \text{ mole)}$$
$$2\chi_{bb} - \chi_{aa} - \chi_{cc} = (9.4 \pm 0.3) \times 10^{-6} \text{ erg/(G}^2 \text{ mole)}$$

[a] Only the relative signs of the molecular g values are determined experimentally. The g values are all shown to have negative signs by other arguments.

five Zeeman parameters. The values of $\langle P_a^2 \rangle$, $\langle P_b^2 \rangle$, and $\langle P_c^2 \rangle$ are evaluated by standard techniques using the previous rotational assignment[6] of $A = 77{,}510.73$ MHz, $B = 12{,}055.03$ MHz, and $C = 10{,}416.21$ MHz. The three g values and two of the susceptibility anisotropy terms are then treated as adjustable parameters in a least-squares fit program giving the results in Table II. The calculated spectra using the Zeeman parameters in Table II are listed in Table I.

Molecular Quadrupole Moments

Hüttner, Lo, and Flygare[4] have given a general expression relating the molecular quadrupole moments to the parameters in Table II. This equation is

$$Q_{zz} = \frac{|e|}{2}\sum_n Z_n(3z_n^2 - r_n^2) - \frac{|e|}{2}\left\langle 0\left|\sum_i (3z_i^2 - r_i^2)\right|0\right\rangle$$
$$= -\frac{\hbar|e|}{8\pi M}\left[\frac{2g_{zz}}{G_{zz}} - \frac{g_{xx}}{G_{xx}} - \frac{g_{yy}}{G_{yy}}\right] - \frac{2mc^2}{|e|N}(2\chi_{zz} - \chi_{xx} - \chi_{yy}) \quad (3)$$

$|e|$ is the electronic charge, Z_n is the charge on the nth nucleus, and z_n and z_i are the nuclear and electronic center of mass coordinates summed over all n nuclei and i electrons. $\langle 0| \; |0\rangle$ indicates the ground electronic state average value. M is the proton mass, $\hbar$ is Planck's constant divided by 2π, G_{zz} is the rotational constant along the zth principal inertial axis, c is the speed of light, m is the electron mass, and N is Avogadro's number. Direct substitution from Table II into eq 3 gives two sets of Q for either choice of the signs of the g values. The b axis bisects the OCO angle, and the a axis is also in the OCO plane and nearly passes through both oxygen atoms (see Figure 4).

g values all negative

$$Q_{aa} = -(5.3 \pm 0.4) \times 10^{-26} \text{ esu cm}^2$$
$$Q_{bb} = +(5.2 \pm 0.4) \times 10^{-26} \text{ esu cm}^2 \quad (4)$$
$$Q_{cc} = +(0.1 \pm 0.4) \times 10^{-26} \text{ esu cm}^2$$

g values all positive

$$Q_{aa} = +(1.5 \pm 0.4) \times 10^{-26} \text{ esu cm}^2$$
$$Q_{bb} = -(15.9 \pm 0.4) \times 10^{-26} \text{ esu cm}^2 \quad (5)$$
$$Q_{cc} = +(14.4 \pm 0.4) \times 10^{-26} \text{ esu cm}^2$$

We can now make a choice for the absolute signs of the g values by comparing the above molecular quadrupole moments with the center of mass quadrupole moments in other molecules. Recent results for several similar molecules are listed in Table III. The x and z axes are the heavy-atom in-plane principal inertial axes.

A quick scan of the above known moments leads to the conclusion that eq 4 gives the correct molecular quadrupole moments in formic acid. Comparing OCO to ketene shows that the large negative z molecular quad-

Table III

Ref	Molecule	Quadrupole moments, 10^{-26} cm^2 esu
a	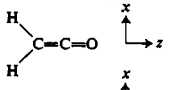	$Q_{zz} = -0.7$ $Q_{xx} = 3.8$
b	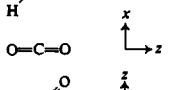	$Q_{zz} = -4.3$ $Q_{xx} = 2.15$
c	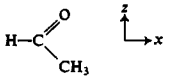	$Q_{zz} = -1.2$ $Q_{xx} = 1.0$
d	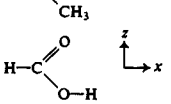	$Q_{zz} = -5.3$ $Q_{xx} = 5.2$

[a] Reference 8. [b] A. D. Buckingham, R. L. Disch, and D. A. Dunmur, *J. Am. Chem. Soc.*, **90**, 3104 (1968). [c] W. Hüttner and W. H. Flygare, unpublished results. [d] Present work.

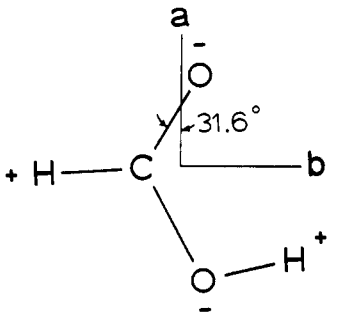

Figure 4. Structure of the formic acid molecule. The bond angles are ∠O–C–O = 124.8°, ∠H–C–O = 111.0°, ∠C–O–H = 105.5°. The bond lengths are H—C = 1.097, C=O = 1.202, C—O = 1.343, O–H = 0.972 Å.

rupole moment is diminished in ketene due to the positive contribution of the protons. Similarly the Q_{xx} values for H_2C_2O and $HCOCH_3$ are positive due to the proton contribution. Thus, we would expect Q_{xx} in formic acid to be positive. The value of $Q_{xx} = -15.9 \times 10^{-26}$ esu cm^2 in eq 5 is therefore unreasonable, which rejects the positive signs for the g values in formic acid. The assignment of the negative signs for the molecular g values in formic acid (eq 5) is also consistent with the known negative signs for the g values in formaldehyde,[4] ketene,[8] acetaldehyde,[9] and carbon dioxide.[5]

The Anisotropies of the Second Moment of the Electronic Charge Distribution

The anisotropies in the center of mass average values of x^2, y^2, and z^2 for the electronic charge distribution are also directly available from the experimental results in Table II and the known molecular structure of formic acid.[10] The structure and orientation of the principal inertial axes are shown in Figure 4.

The total magnetic susceptibility, χ_{xx}, along any axis is a sum of diamagnetic, χ_{xx}^{d}, and paramagnetic, χ_{xx}^{p}, components defined by[11]

$$\chi_{xx} = \chi_{xx}^{p} + \chi_{xx}^{d}$$

$$\chi_{xx}^{d} = \frac{-e^2N}{4mc^2}\left\langle 0\left|\sum_i (y_i^2 + z_i^2)\right|0\right\rangle \qquad (6)$$

$$\chi_{xx}^{p} = \frac{-e^2N}{6mc^2}\left[\frac{\hbar g_{xx}}{8\pi G_{xx}M} - \frac{1}{2}\sum_n Z_n(y_n^2 + z_n^2)\right]$$

We now define the average values of the second moment of the electronic charge distributions as

$$\langle x^2\rangle = \left\langle 0\left|\sum_i x_i^2\right|0\right\rangle$$

$$\langle y^2\rangle = \left\langle 0\left|\sum_i y_i^2\right|0\right\rangle \qquad (7)$$

$$\langle z^2\rangle = \left\langle 0\left|\sum_i z_i^2\right|0\right\rangle$$

Returning to eq 6, we can relate the anisotropies of the second moments in eq 7 to the observables in Table II and the known molecular structure.[10] The appropriate equation is

$$\langle y^2\rangle - \langle x^2\rangle = \sum_n Z_n(y_n^2 - x_n^2) + \frac{\hbar}{4\pi M}\left(\frac{g_{yy}}{G_{yy}} - \frac{g_{xx}}{G_{xx}}\right) + \frac{4mc^2}{3e^2N}[(2\chi_{yy} - \chi_{xx} - \chi_{zz}) - (2\chi_{xx} - \chi_{yy} - \chi_{zz})] \qquad (8)$$

The results are (the c axis is perpendicular to the molecular plane as shown in Figure 4)

$$\langle a^2\rangle - \langle b^2\rangle = (17.8 \pm 0.3) \times 10^{-16}\ \text{cm}^2$$
$$\langle a^2\rangle - \langle c^2\rangle = (22.1 \pm 0.3) \times 10^{-16}\ \text{cm}^2 \qquad (9)$$
$$\langle b^2\rangle - \langle c^2\rangle = (4.3 \pm 0.3) \times 10^{-16}\ \text{cm}^2$$

Magnetic Susceptibility and Individual Elements in the Second Moment of the Charge Distribution

Each of the individual elements of the second moment of the electronic charge distribution can be obtained by using the bulk magnetic susceptibility. Broersma[12] has measured the bulk magnetic susceptibility in liquid formic acid. The result is

$$\chi = \frac{1}{3}(\chi_{aa} + \chi_{bb} + \chi_{cc})$$
$$= -(19.9 \pm 0.3) \times 10^{-6}\ \text{erg}/(\text{G}^2\,\text{mole}) \qquad (10)$$

If we assume that χ(liquid) = χ(gas) we can combine the above bulk value with the anisotropies in Table II to obtain the individual diagonal elements in the magnetic susceptibility tensor. The results are (in units of erg/(G^2 mole))

$$\chi_{aa} = -(18.8 \pm 0.8) \times 10^{-6}$$
$$\chi_{bb} = -(16.8 \pm 0.8) \times 10^{-6} \qquad (11)$$
$$\chi_{cc} = -(24.2 \pm 0.8) \times 10^{-6}$$

Furthermore, we can also list the diagonal elements in the paramagnetic susceptibility tensor from eq 6, the known molecular structure, and the g values in Table II. These results are listed in Table IV. The diagonal elements in the diamagnetic susceptibility tensor are also listed in Table IV (see eq 6).

We can now compute the individual elements in second moment of the electronic charge distribution. These results are

$$\langle a^2\rangle = (25.6 \pm 0.3) \times 10^{-16}\ \text{cm}^2$$
$$\langle b^2\rangle = (7.7 \pm 0.3) \times 10^{-16}\ \text{cm}^2 \qquad (12)$$
$$\langle c^2\rangle = (3.5 \pm 0.3) \times 10^{-16}\ \text{cm}^2$$

Discussion

A complete description of the diagonal elements in the magnetic susceptibility tensor has been obtained in formic acid in the principal inertial axis system. The diagonal elements in total magnetic susceptibility tensor of $\chi_{aa} = -18.8$, $\chi_{bb} = -16.8$, and $\chi_{cc} = -24.2$ are similar to the corresponding principal inertial axes values in acetaldehyde of $\chi_{aa} = -20.0$, $\chi_{bb} = -19.5$, $\chi_{cc} = -28.6$ (all in units of 10^{-6} erg/(G^2 mole)).

(9) W. Hüttner and W. H. Flygare, unpublished results.
(10) G. H. Kwei and R. F. Curl, *J. Chem. Phys.*, **32**, 1592 (1960).
(11) W. H. Flygare, *ibid.*, **42**, 1563 (1965).
(12) S. Broersma, *ibid.*, **17**, 873 (1949).

Table IV. The Diagonal Elements in the Total, χ_{xx}, Paramagnetic, χ_{xx}^{P}, and Diamagnetic, χ_{xx}^{d}, Susceptibility Tensor in the Principal Inertial Axis System in Formic Acid[a]

Principal inertial axis	Total	Paramagnetic	Diamagnetic
a	$-(18.8 \pm 0.8)$	28.8 ± 0.1	$-(47.6 \pm 0.8)$
b	$-(16.8 \pm 0.8)$	106.5 ± 0.1	$-(123.3 \pm 0.8)$
c	$-(24.2 \pm 0.8)$	117.2 ± 0.1	$-(141.4 \pm 0.8)$

[a] The units are 10^{-6} erg/(G^2 mole).

The in-plane molecular quadrupole moments in formic acid are the largest values known at this time. The large negative value is along a line which passes approximately through both oxygen atoms. The large positive value is along a line which passes near to both hydrogen atoms. Thus, it is evident that the negative charge builds up at the oxygen extremities, and the positive charge shows up at the hydrogen extremities. This interpretation is consistent with the results on similar molecules.

The average values of a^2, b^2, and c^2 are also interesting to compare with other molecules. As formic acid is planar, the average value of c^2 gives a direct indication of the out-of-plane electron density. The value of $\langle c^2 \rangle = (3.5 \pm 0.3) \times 10^{-16}$ cm^2 is compared in Table V to other molecules.

Table V

Ref	Molecule	Out-of-plane (off-axis) value of $\langle x^2 \rangle$, 10^{-16} cm^2
This work	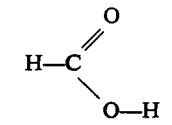	3.5
a	N—N—O	3.0
a	O—C—O	3.0
5	O—C—S	4.5
b	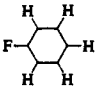	8.4

[a] R. Shoemaker, W. Hüttner, and W. H. Flygare, *J. Chem. Phys.*, in press. [b] W. Hüttner and W. H. Flygare, *ibid.*, in press.

Acknowledgment. The support of the National Science Foundation is gratefully acknowledged.

The Microwave Spectrum, Structure, and Dipole Moment of *cis*-Thionylimide

William H. Kirchhoff

Contribution from the National Bureau of Standards, Washington, D. C. 20234.
Received August 12, 1968

Abstract: The microwave spectrum of thionylimide, HNSO, has been observed and assigned to the planar *cis* form. The structural parameters are $d_{NH} = 1.029 \pm 0.01$ Å, $d_{NS} = 1.512 \pm 0.005$ Å, $d_{SO} = 1.451 \pm 0.005$ Å, $\angle HNS = 115.8 \pm 1°$, and $\angle NSO = 120.4 \pm 0.5°$, where the uncertainties are estimated to account for the effects of zero-point vibrations. The dipole moment and its components along the principal axes in the HN^{15}SO isotopic species are $\mu_a = 0.893 \pm 0.003$ D, $\mu_b = 0.181 \pm 0.005$ D, and $\mu = 0.911 \pm 0.003$ D, where the uncertainties are the standard deviations of the reported values, from the least-squares analysis. Since no attempts were made to make a complete assignment of the impure sample, no comments can be made about the possible existence of *trans*-HNSO.

Thionylimide, HNSO, was first prepared by Schenk[1] by treating NH_3 with $SOCl_2$ and was later investigated by Becke-Goehring, Schwarz, and Spiess[2] who suggested a structure analogous to SO_2 with an NH group replacing one of the oxygen atoms. Most recently, Richert[3] has carried out a study of the infrared spectrum of HNSO, confirming the SO_2-like structure and obtaining valence force constants, bond orders, and estimates of the bond angles.

During the investigation of the microwave spectrum of NSF reported in a previous paper,[4] it was found that the appearance of certain transitions in the microwave spectrum could be correlated with certain peaks in the mass spectrum. The mass spectral cracking pattern suggested that the impurity might be HNSO. Richert and Glemser[5] have reported that HNSO is formed as an intermediate product in the hydrolysis of NSF. Hydrolysis experiments carried out in the mass spectrometer and the microwave absorption cell confirmed this.

Although a previous study of HNSO yielded a tentative structure[4] and showed that the conformation of HNSO

(1) P. W. Schenk, *Ber.*, **65**, 94 (1942).
(2) M. Becke-Goehring, R. Schwarz, and W. Spiess, *Z. Anorg. Allg. Chem.*, **293**, 294 (1958).
(3) H. Richert, *ibid.*, **309**, 171 (1961).
(4) W. H. Kirchhoff, Ph.D. Thesis, Harvard University, Cambridge, Mass., 1962, pp III-1, 28.
(5) O. Glemser and H. Richert, *Z. Anorg. Allg. Chem.*, **307**, 313 (1961).